Research Article

A Sensitive Fluorescent Immunoassay for Prostate Specific Antigen Detection Based on Signal Amplify Strategy of Horseradish Peroxidase and Silicon Dioxide Nanospheres

Lihua Li [ORCID],[1] Wenzhi Zhang,[1] Yan Wei,[1,2] Lizhen Yu [ORCID],[1] and Dexiang Feng [ORCID] [1,2]

[1]*Department of Pharmacy, Wannan Medical College, Wuhu 241002, China*
[2]*Institute of Synthesis and Application of Medical Materials, Department of Chemistry, Wannan Medical College, Wuhu 241002, China*

Correspondence should be addressed to Lizhen Yu; yulizhen@wnmc.edu.cn and Dexiang Feng; fengdxiang@163.com

A simple, sensitive, and fluorescent immunoassay for the detection of prostate-specific antigen (PSA) based on horseradish peroxidase and silicon dioxide nanospheres as a signal amplification strategy has been described. In the design, the primary antibody (Ab_1) of PSA was first immobilized on the 96-well plates via physical adsorption between polystyrene and hydrophobic groups of the antibody molecule. The silicon dioxide nanospheres (SiO_2 NSs), with large surface area and good biocompatibility, were loaded with horseradish peroxidase (HRP) and horseradish peroxidase-labeled secondary antibodies (HRP-Ab_2) as signal amplification systems. In the presence of PSA, a sandwich-type immunocomplex composed of Ab_1-Ag-HRP-Ab_2 had been formed. Fluorescence technology was employed to obtain the response signal of the immunoassay in the *L*-tyrosine and H_2O_2 systems. Experiment results showed that a strong and stable fluorescent signal at 416 nm (excitation wavelength: 325 nm) was observed, and the changes in fluorescent intensity were related to the levels of PSA. Under the optimal conditions, the relative fluorescence intensity was linear with the logarithm of PSA concentration from 0.03 to 100 ng·mL^{-1}, with a detection limit of 0.01 ng·mL^{-1} (at a signal/noise ratio of 3). In contrast to other fluorescent immunoassays, the sandwich-type immunoreaction based on the high binding ELISA plates has the advantages of being simple, stable, and easy to operate, high selectivity, small sample quantity, etc., which can be widely used in the selective detection of a variety of targets, from DNA to proteins and small molecules. Such fluorescent immunoassays should be feasible for the fields of molecular diagnosis and other life science fields in the future.

1. Introduction

Prostate cancer now ranks as one of the most prevalent health killers among males worldwide [1]. In particular, the percentages of patients in China with aggressive prostate cancer and survival rates are unpromising compared with those in western countries [2]. Prostate-specific antigen (PSA), a glycoprotein almost entirely secreted by the prostate gland, is considered to be one of the most reliable clinical biomarkers for the diagnosis, screening, and risk prediction of prostate cancer, and it was the first tumor biomarker approved by the Food and Drug Administration (FDA) [3, 4]. For healthy individuals, the serum PSA level is extremely low, about 4.0 ng·mL^{-1} and more than 10 ng·mL^{-1}, making them prone to developing prostate cancer [5–7]. Therefore, the sensitive and accurate detection of serum PSA is critical for monitoring early asymptomatic prostate cancer, increasing the chances of cure and reducing its mortality.

In order to obtain ideal methods for PSA testing, scientists have proposed a series of biosensing strategies, and immunoassay was initially favored [8]. Based on the specific interaction between PSA and its antibody, immunoassays have made many achievements in PSA detecting strategies, including radioimmunoassay (RIA), enzyme-linked immunosorbent assays (ELISA), and electrophoretic

immunoassay [9, 10]. The detection results of these methods are reliable. However, these methods need complex procedures and a long time. In recent years, electrochemical and optical immunoassay methods have been developed for PSA detection [11, 12]. Although low detection limits are achieved using electrochemical immunoassay, the reproducibility of electrochemical immunoassay is still a challenge. Moreover, undesired biomolecules in serum may produce interference with the detected objects. Optical immunoassays, including fluorescence (FL) [13], surface plasmon resonance (SPR) [14], chemiluminescence (CL) [15], electrochemiluminescence (ECL) [16], and surface-enhanced Raman spectroscopy (SERS) [17], overcome the disadvantages of interference. Amongst them, fluorescent immunoassay has received considerable attention due to its speed, sensitivity, and signal stability and provides a possible highly sensitive and selective determination of tumor markers at an earlier stage of disease development.

On the other hand, the growing need for early and ultrasensitive surveillance of disease-related biomarkers is driving the development of biomarker-sensitive assays through signal amplification. Fortunately, recent achievements in nanomaterials and nanotechnology have provided new avenues to develop novel signal amplification strategies for ultrasensitive immunoassays [18–20]. Because of their small size, large specific surface area, and good stability at high temperatures, nanoparticles have been widely used for signal amplifications including colloidal gold nanoparticles, magnetic nanoparticles, carbon nanospheres, quantum dots, silicon dioxide nanospheres (SiO_2 NSs), etc. [21–25]. More importantly, the surfaces of these nanoparticles can be modified with oligonucleotides, enzymes, or antibodies to generate biological conjugates that serve as analysis cores and enhance signal generation by producing a synergistic effect to achieve higher sensitivity and lower detection limits [26, 27]. Compared with a variety of nanoparticles, SiO_2 NSs and their nanocomposites serving as signal amplification systems have many advantages: (i) they are nontoxic and highly biocompatible with biological systems; (ii) easy to prepare and their surface can be functionally treated as needed; (iii) the performance is very stable; and (iv) lack of fluorescence quenching as noble metal, magnetic, and carbon nanomaterials [28–30].

In the present study, a sensitive and simple fluorescent immunoassay was designed for the detection for PSA. The primary antibody (Ab_1) of PSA was first immobilized on the 96-well plates. SiO_2 NSs was used as a carrier for the immobilization of HRP and HRP labeled secondary antibody (HRP-Ab_2). In the presence of PSA, the immunocomplex was formed via specific recognition of antibody and antigen. The experimental results showed the introduction of SiO_2 NSs clearly improved the immobilized amount of HRP, Ab_2, and the fluorescent intensity of the system. In addition, the immunoassay method had a wide linear range and high sensitivity. The results were in good agreement with the reference values when the serum samples were detected by our developed method.

2. Materials and Methods

2.1. Materials and Chemicals.
The 96-strips high binding ELISA plates, horseradish peroxidase-labeled monoclonal anti-PSA antibody (HRP-Ab_2), and PSA ELISA kit were purchased from Biocell Co., Ltd., China. Horseradish peroxidase (HRP), Bovine serum albumin (BSA), 3-Aminopropyltriethoxysilane (APTES), Tetraethoxysilane (TEOS), N-hydroxysuccinimide (NHS), 1-ethyl-3-(3-dimethylaminopropyl) carbodiimide hydrochloride (EDC) were purchased from Aladdin Chemistry Co., Ltd., China. All other reagents were analytical grade and purchased from Sinopharm Chemical Reagent Co., Ltd., China. The clinical serum samples were collected from the clinical laboratory of the Yiji Shan Hospital with the consent of the patient. Twice-quartz-distilled water was used throughout the study. All experiments were performed in compliance with the relevant laws and institutional guidelines of the Ethics Committee.

2.2. Devices.
The morphology and size of SiO_2 NSs were measured on a transmission electron microscope (TEM, Hitachi-800, Japan). FTIR spectra of SiO_2 NSs and functionalization were measured on an IR-21 spectrometer (Shimadzu, Japan). The UV-vis absorption spectra were measured on a U-5100 UV-vis-NIR spectrometer (Hitachi, Japan). An electrochemical impedance spectroscopy (EIS) analysis was carried out on the CHI650C three-electrode electrochemical working system. All fluorescence measurements were performed on an F-4600 fluorescence spectrophotometer (Hitachi, Japan).

2.3. Preparation and Functionalization of SiO_2 NSs.
The silicon dioxide nanospheres (SiO_2 NSs) were prepared according to the modified Stöber method [31]. Briefly, 2.3 mL of TEOS was added to a mixture containing 90.0 mL ethanol, 2.7 mL ammonium hydroxide, and 5.0 mL deionized water, and reacted for 24 h under stirring. The silica colloidal dispersion was rinsed three times with ethanol and dried at 37°C to obtain monodisperse SiO_2 NSs. 0.02 g of bare SiO_2 NSs was then dispersed in 50 mL of ethanol and treated with 0.4 mL of APTES. After being stirred for 6 h, the suspension was centrifuged and rinsed three times with ethanol, and the amino-functionalized SiO_2 NSs (NH_2-SiO_2 NSs) were obtained.

SiO_2 NSs with functionalized carboxyl (COOH-SiO_2 NSs) were prepared according to the reported procedure previously with a slight modification [32]. Namely, NH_2-SiO_2 NSs (20 mg) were suspended in 20.0 mL of N, N-Dimethylformamide (DMF) containing 0.1 mol·L^{-1} glutaric anhydride by ultrasonic stirring for 10 min and reacted 24 h under stirring. The resulting suspension was centrifuged, and the sediments were then washed three times alternately with DMF and deionized water.

2.4. Preparation of HRP-Ab_2-SiO_2 NSs Bioconjugate.
First, the COOH-SiO_2 NSs (20.0 mg) were suspended in 2.0 mL of PBS (pH 7.4) and ultrasonically stirred for 10 min to obtain a
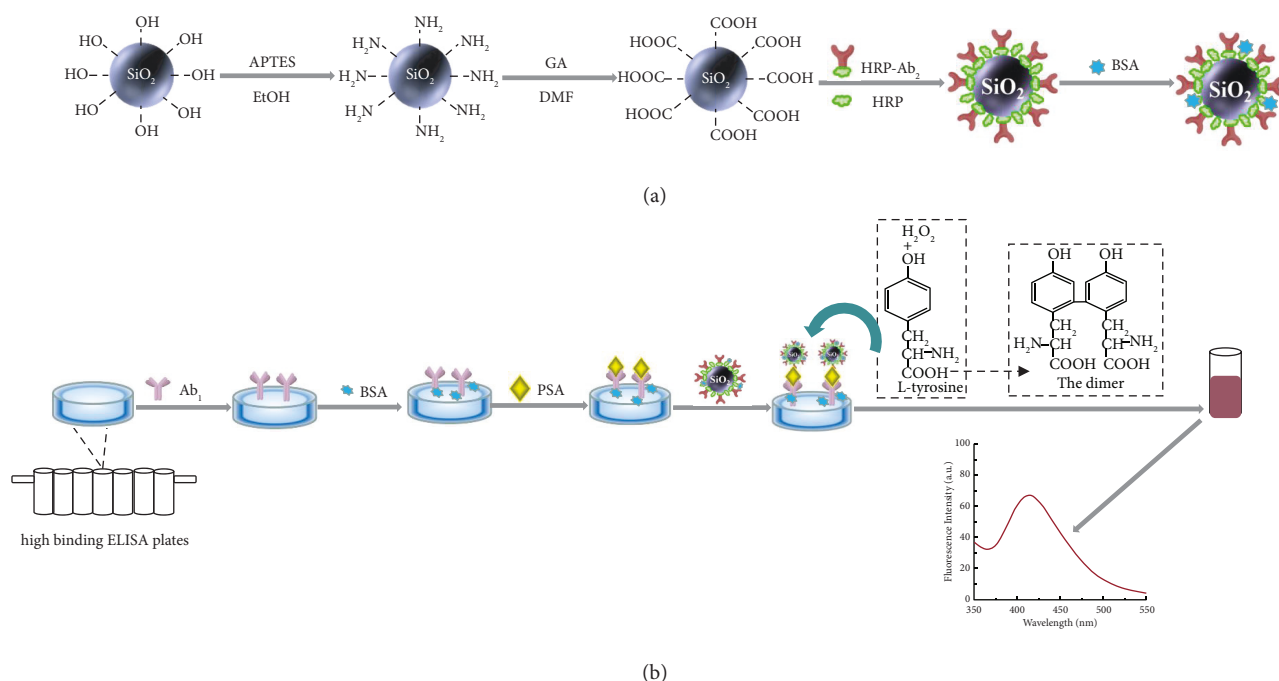
(a)

(b)

FIGURE 1: (a) Schematic illustration of the fabrication of HRP-Ab$_2$-SiO$_2$ NSs bioconjugate. (b) The construction process of the immunoassay for fluorescence detection of PSA.

homogeneous dispersion. Then, 2.6 mg of EDC and 2.6 mg of NHS were added into the mixture above and activated for 30 min. Subsequently, 0.1 mL of HRP-Ab$_2$ (1.0 mg·mL^{-1}) and 0.3 mL of HRP (0.5 mg·mL^{-1}) were added to the dispersion and stirred overnight at room temperature. The excess HRP-Ab$_2$ and HRP were removed by centrifugation (10,000 rpm, 10 min). After being rinsed with PBS (pH 7.4), the resulting mixture was redispersed in 2.0 mL of PBS containing 1% BSA and stored at 4°C for further use. The schematic illustration of the preparation of the HRP-Ab$_2$-SiO$_2$ NSs bioconjugate is shown in Figure 1(a).

2.5. Detection of PSA. A sandwich-type immunoassay protocol was used for the detection of PSA as shown in Figure 1(b). First, 80.0 μL of 100.0 ng·mL^{-1} PSA primary antibodies (Ab$_1$) were added to the 96-well plates and placed overnight at 4°C. These wells were washed with PBS to remove unbound antibodies. Then 1% BSA was added to each well at 37°C for 45 min to block excessive binding sites. Second, 80.0 μL of PSA with different concentrations was added to each well. After incubation for 1 h at 37°C, these wells were washed three times with PBS to remove the unbound antigens. Third, 80 μL of the HRP-Ab$_2$-SiO$_2$ NSs bioconjugate was added to the wells and incubated for 1 h at 37°C. Finally, 240.0 μL of Tris-HCL buffer solution (pH 7.4), 40 μL of 55 μM L-tyrosine, and 2.0 μL of 0.003% H$_2$O$_2$ (5 μM) were added to each well, respectively. After 30 min, the fluorescent intensity of the solution was measured.

3. Results and Discussion

3.1. Preparation and Functionalization of SiO$_2$ NSs. In this study, TEM and FTIR were used to investigate the shape of

SiO$_2$ NSs obtained and their functionalization. Figure 2(a) showed a TEM image of the SiO$_2$ NSs. It could be observed that the SiO$_2$ NSs had a uniform spherical shape with an average size of ~140 nm in diameter. In the experiment, we found that the SiO$_2$ NSs could be easily centrifuged, which facilitated the separation process after enzyme and antibody functionalization.

Surface modification of SiO$_2$ NSs was often used in immunoassays. As a silylating reagent, APTES reacted with the silanol groups from SiO$_2$ NSs to introduce amino groups to the surface of SiO$_2$ NSs. The carboxylic groups were then obtained by a ring opening linker elongation reaction between the amino group and glutaric anhydride.

The FTIR spectrum of SiO$_2$ NSs (Figure 2(b), black curve) displayed the presence of the asymmetrical Si-O-Si vibration (1103 cm^{-1}). In addition, there were two vibration absorptions associated with Si-O-Si at 798 cm^{-1} and 463 cm^{-1}, accompanied by a broad band in the range of 3100–3700 cm^{-1} of the OH stretching. In the FTIR spectrum of NH$_2$-SiO$_2$ NSs (Figure 2(b)), red curve), besides the absorption caused by Si-O vibrations, the weak peak at 2938 cm^{-1} was considered to be the C-H stretching vibration of the CH$_2$ groups, and the 1512 cm^{-1} absorption was attributed to δ_{NH} of the NH$_2$ groups, both of which are associated with the APTES skeleton. The signal broadening in the range of 3100–3700 cm^{-1} was attributed to an envelope of OH signal from adsorbed water, silanol, and N-H stretching vibration of the amino groups [33]. Compared with that of SiO$_2$ NSs, the FTIR spectrum of the COOH-SiO$_2$ NSs (Figure 2(b), blue curve) displayed a strong peak at 1682 cm^{-1}, which confirmed the presence of a carboxyl group. These data indicated that the functionalization of SiO$_2$ NSs with carboxyl groups was successful.
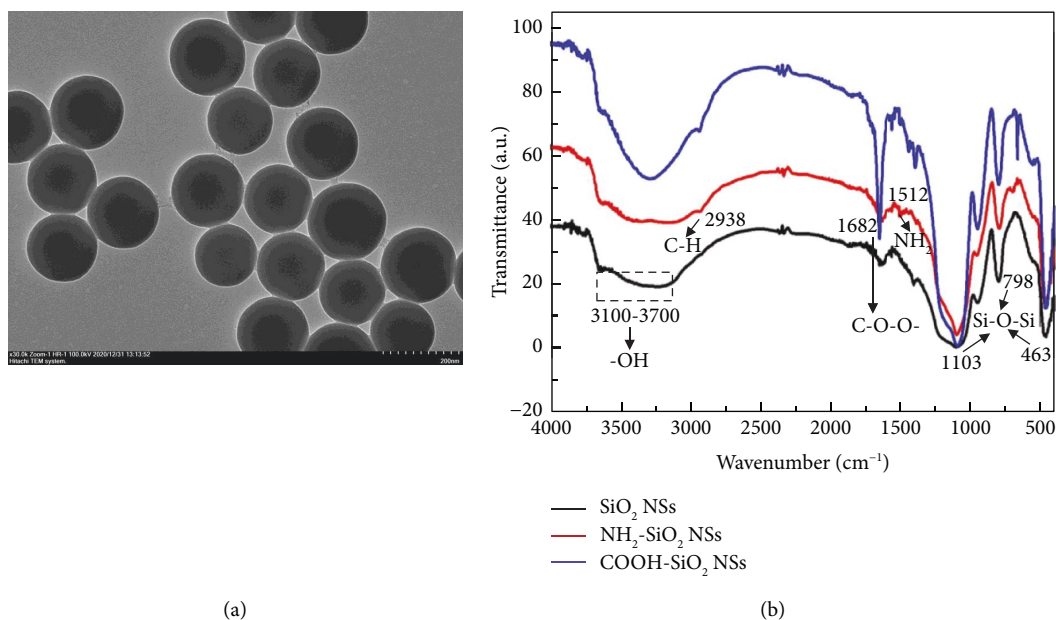
(a)

(b)

Figure 2: (a) TEM image of SiO_2 NSs. (b) FTIR spectra of SiO_2 NSs, NH_2-SiO_2 NSs, and COOH-SiO_2 NSs.

3.2. Characterizations of HRP-Ab_2-SiO_2 NSs Bioconjugate.

First, UV-vis spectrophotometry was used to characterize the HRP-Ab_2-SiO_2 NSs bioconjugates. From Figure 3(a), it could be observed that the bioconjugate appeared with two new obvious absorptive peaks at 280 nm and 402 nm, which came from Ab_2 and HRP, indicating that HRP-Ab_2 and HRP were successfully bonded to SiO_2 NSs via the EDC/NHS method.

Then, the ninhydrin reaction was adopted to verify the presence of antibodies in the bioconjugate. A ninhydrin reaction is a chemical reaction in which a substance containing a free amino group, such as an amino acid, protein, or polypeptide, reacts with ninhydrin in the presence of heat and a weak acid to produce a specific-colored substance. An antibody is a protein with a unique structure that enables it to bind specifically to its corresponding antigen [34]. There are abundant amino groups and carboxyl groups in the basic structure of antibodies. As can be seen from Figure 3(b), the surface of NH_2-SiO_2 NSs was rich in amino groups, which reacted with ninhydrin to produce dark purple products. Compared with NH_2-SiO_2 NSs, HRP-Ab_2 and HRP-Ab_2-SiO_2 NSs bioconjugates also contained amino groups, but fewer free amino groups, and the product color was light purple. The experimental results showed that antibodies were successfully modified on the surface of SiO_2 NSs.

At the same time, electrochemical impedance spectroscopy (EIS) was also employed to characterize the bioconjugate. The EIS consists of a linear section representing the diffusion limiting process and a semicircular section reflecting the size of the electron transfer resistance (Ret) [35]. In comparison with the bare glassy carbon electrode (GCE, Ret about 200 Ω, Figure 3(c)) (A), the electron transfer was blocked when GCE was modified by SiO_2 NSs due to poor conductivity, and the Ret value increased to 416 Ω (Figure 3(c)) (B). Meanwhile, it can be observed that the

impedance was further improved after GCE was decorated with HRP-Ab_2-SiO_2 NSs bioconjugate, suggesting that the addition of antibody hindered the efficiency of the electron transfer between the electrode and the solution, which also indirectly proved that antibodies were successfully modified on the surface of SiO_2 NSs (Figure 3(c)) (C).

3.3. Optimization of Immunoassay Conditions for PSA Detection.

It is well known that the results of an immunoassay are influenced by many factors, including pH and reaction time. In order to obtain excellent analytical performance, some experiment conditions were optimized. Since the pH of the solution affected HRP activity, L-tyrosine solubility, and antibody stability, we investigated the effect of pH on the immunoassay. Figure 4(a) showed the effect of pH on the fluorescent intensity. An increase in fluorescence intensity, followed by a decline, was clearly observed as pH increased from 6.0 to 8.0. In this work, we selected a solution with a pH of 7.4 because it was close to the physiological pH value and the fluorescent intensity was relatively high at pH 7.4.

The concentration of H_2O_2 was a very important factor affecting the performance of the immunoassay. Low concentration resulted in an unsatisfactory performance of the immunoassay. At high concentration, horseradish peroxidase activity declined. The experiment result showed that the fluorescent intensity reached the maximum when the concentration of H_2O_2 was $5\,\mu M$ (Seen in Figure 4(b)). Therefore, $5\,\mu M$ of H_2O_2 was selected in this work.

At the same time, we investigated the different ratios of HRP-Ab_2-SiO_2 NSs bioconjugated to L-tyrosine because it would directly affect the signal intensity of the immunoassay. In this work, the fluorescent intensity was mainly dependent on the catalytic effect of captured HRP on
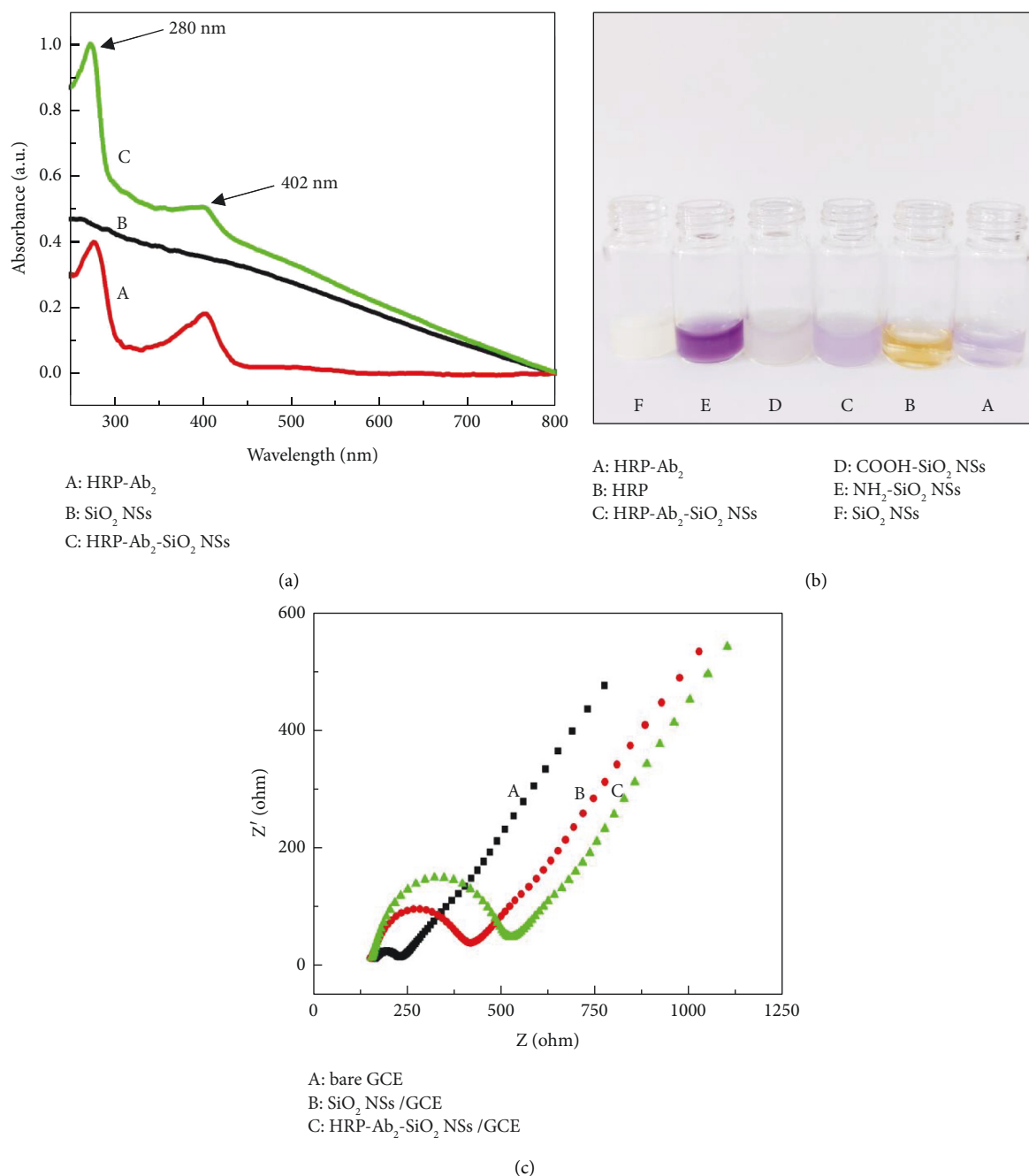
(a)

A: HRP-Ab$_2$
B: SiO$_2$ NSs
C: HRP-Ab$_2$-SiO$_2$ NSs

(b)

A: HRP-Ab$_2$
B: HRP
C: HRP-Ab$_2$-SiO$_2$ NSs
D: COOH-SiO$_2$ NSs
E: NH$_2$-SiO$_2$ NSs
F: SiO$_2$ NSs

A: bare GCE
B: SiO$_2$ NSs /GCE
C: HRP-Ab$_2$-SiO$_2$ NSs /GCE

(c)

Figure 3: (a) UV-vis absorption of (A) HRP-Ab$_2$, (B) SiO$_2$ NSs, and (C) HRP-Ab$_2$-SiO$_2$ NSs. (b) Ninhydrin color reaction of (A) HRP-Ab$_2$, (B) HRP, (C) HRP-Ab$_2$-SiO$_2$ NSs, (D) COOH-SiO$_2$ NSs, (E) NH$_2$-SiO$_2$ NSs, and (F) SiO$_2$ NSs. (c) EIS spectra of (A) bare GCE, (B) SiO$_2$ NSs/GCE, and (C) HRP-Ab$_2$-SiO$_2$ NSs/GCE.

L-tyrosine. If HRP content was too low, it was not enough to completely catalyze L-tyrosine, and if HRP content was too high, it would cause unnecessary waste. As can be seen from Figure 4(c), the fluorescent intensity gradually increased and then remained stable as the ratio of HRP-Ab$_2$-SiO$_2$ conjugate to L-tyrosine from 1 : 4 to 2 : 1. Therefore, the ratio of 2 : 1 was selected in the study, namely 80 μL of the HRP-Ab$_2$-SiO$_2$ NSs bioconjugate and 40 μL of 55 μM L-tyrosine.

The effect of the reaction time on signal intensity was also investigated. As shown in Figure 4(d), the fluorescent

intensity displayed its maximum when the reaction time reached 30 min and kept a stable value for 2 h at room temperature. Thus, the fluorescent measurements were carried out when the reaction time was 30 min.

3.4. Analytical Performance. The quantitative range of the immunoassay was assessed under optimum conditions. The results in Figure 5 showed that the fluorescent intensity increased gradually with the increase of PSA concentration,
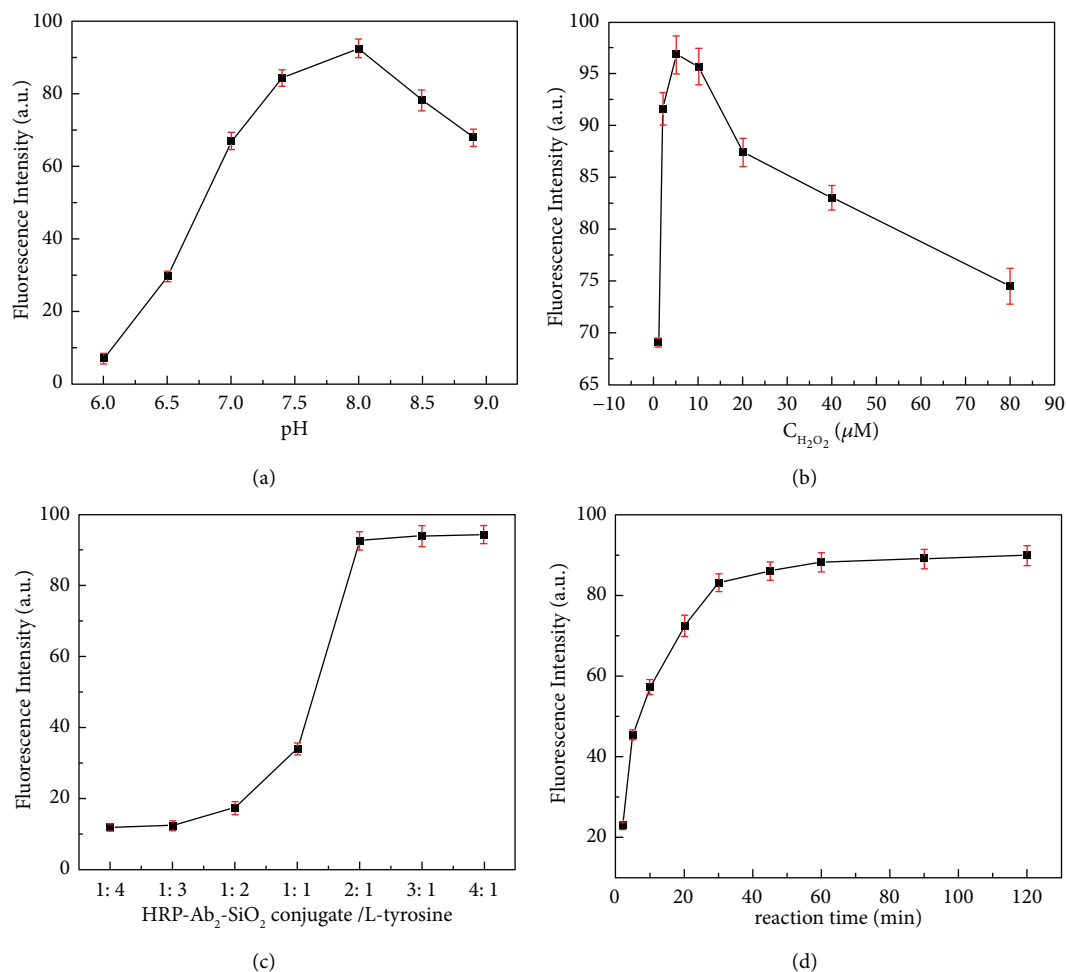
(a)

(b)

(c)

(d)

FIGURE 4: Effects of (a) pH, (b) the concentration of H_2O_2, (c) the ratios of HRP-Ab_2-SiO_2 NSs bioconjugate to L-tyrosine (v/v, L-tyrosine concentration:55 μM), and (d) the reaction time on the fluorescent intensity of the immunoassay with PSA antigen concentration of 50 ng·mL^{-1} (error bars represent standard deviations from three repeated measurements).

(a)

(b)
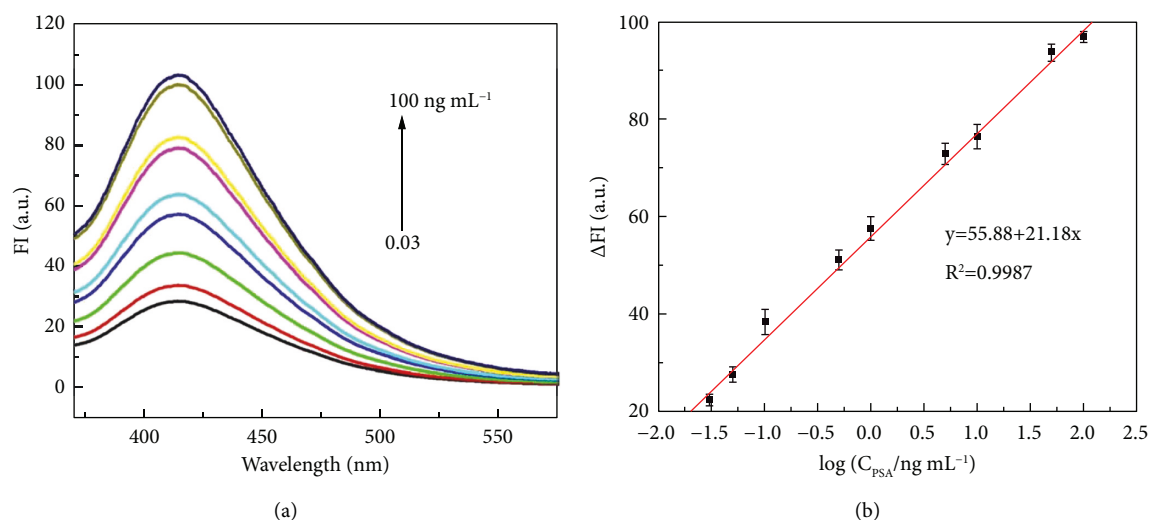
FIGURE 5: (a) Fluorescence spectra of immunoassays with a target PSA concentration of 0.03, 0.05, 0.1, 0.5, 1, 5, 10, 50, 100 ng·mL^{-1} from the bottom spectrum to the top spectrum. (b) The calibration plot of relative fluorescence intensity (ΔFI) vs. the logarithm of PSA concentration (error bars represent standard deviations from three repeated measurements).
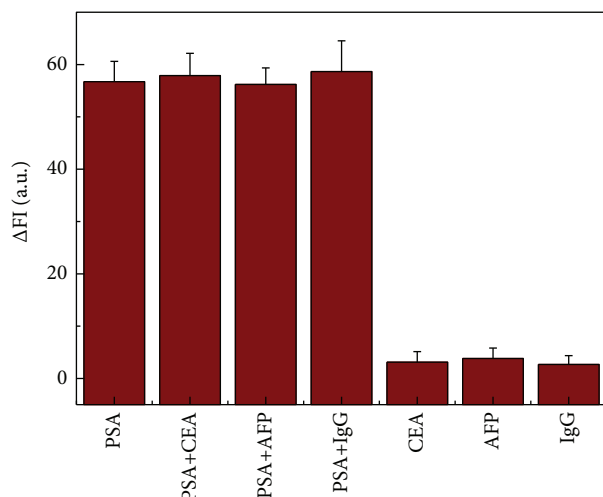
FIGURE 6: Specificity for PSA determination in the developed immunoassay. The concentration of PSA was $1.0 \, \text{ng·mL}^{-1}$, and the concentration of the other antigens was $10.0 \, \text{ng·mL}^{-1}$.

and a good calibration curve was obtained in the range of 0.03 to $100 \, \text{ng·mL}^{-1}$ $y = 55.88 + 21.18x$ was a linear regression equation, and its linear regression coefficient was 0.9987. The detection limit was estimated to be $0.01 \, \text{ng·mL}^{-1}$ (S/N = 3). The reason for the high sensitivity of this method may be attributed to the large specific surface area of SiO_2 NSs for loading the amount of HRP and antibodies to amplify the response signal.

3.5. Specificity for PSA Detection. To verify the specificity of the proposed immunoassay method, similar target antigens, such as carcinoembryonic antigen (CEA), a-fetoprotein (AFP), and immunoglobulin *G* (IgG), were employed to investigate interference by monitoring the changes in the immune response signal. As shown in Figure 6, the signal produced by the non-specific antigen was negligible compared to the target antigen. The specificity of the immunoassay depends mainly upon the antibodies involved in the immune reaction. The sandwich technique with two kinds of antibodies (Ab_1 and Ab_2) further improved the specificity of the proposed method [36].

3.6. Samples Analysis. To examine the applicability of the developed immunoassay method in serum sample analysis, different quantities of known concentrations of PSA were added into the serum of healthy people for a sample recovery experiment. The results obtained were summarized in Table 1. It could be observed that the recoveries were within 96.1–105.0%, indicating that the proposed method had acceptable accuracy.

In order to further explore the feasibility of the clinical application of this method, eight human serum samples from Yiji Shan Hospital (Wuhu, China) were detected by the proposed and ELISA methods. The results were compared with the reference values obtained from the ELISA method (seen in Table 2). The relative deviations were within −5.22% to 4.16%, indicating that the results obtained by the

TABLE 1: Recovery results of PSA in human serum samples ($n = 9$).

Serum sample	Added (ng·mL^{-1})	Found[a] (ng·mL^{-1})	Recoveries (%)
1	0.03	0.0315	105.0
2	0.05	0.0521	104.2
3	0.1	0.1026	102.6
4	0.5	0.4805	96.1
5	1.0	0.9881	98.8
6	5.0	4.9558	99.1
7	10.0	10.214	102.1
8	50.0	48.786	97.6
9	100.0	96.366	96.4

[a]Mean value ± SD of five measurements serum sample.

TABLE 2: Comparison results of serum samples using the proposed and ELISA method.

Serum sample	Proposed method[a] (ng·mL^{-1})	ELISA[a] (ng·mL^{-1})	Relative deviation (%)
1	1 0.116 ± 0.012	0.113 ± 0.008	2.65
2	2 0.308 ± 0.018	0.316 ± 0.014	−2.53
3	0.653 ± 0.011	0.689 ± 0.015	−5.22
4	1.152 ± 0.009	1.138 ± 0.021	1.23
5	5.210 ± 0.025	5.002 ± 0.034	4.16
6	15.262 ± 0.138	14.806 ± 0.112	3.08
7	24.139 ± 0.165	25.418 ± 0.104	−5.03
8	43.615 ± 0.213	42.221 ± 0.226	3.30

[a]Mean value ± SD of five measurements serum sample.

proposed immunoassay were in agreement with those obtained by the ELISA.

4. Conclusions

In conclusion, a simple fluorescent immunoassay for PSA detection has been designed based on the signal amplification of HRP conjugated by SiO_2 NSs. SiO_2 NSs with large surface areas were loaded with more horseradish peroxidase (HRP) to speed up the catalytic process of HRP toward H_2O_2, which effectively amplified detection signals. The immunoassay exhibited high sensitivity and provided promising potential in clinical applications.

Data Availability

No additional data were used to support this study.

Conflicts of Interest

The authors declare that they have no conflicts of interest.

Acknowledgments

References

[1] S. Z. Chen, L. Xu, K. Sheng et al., "A label-free electrochemical immunosensor based on facet-controlled Au nanorods/reduced graphene oxide composites for prostate specific antigen detection," *Sensors and Actuators B: Chemical*, vol. 336, Article ID 129748, 2021.

[2] Y. Jiang, X. F. Chen, N. H. Feng, and P. Miao, "A highly sensitive aptasensor for the detection of prostate specific antigen based on dumbbell hybridization chain reaction," *Sensors and Actuators B: Chemical*, vol. 340, Article ID 129952, 2021.

[3] D. C. Pérez-Ibave, C. H. Burciaga-Flores, and M. Á. Elizondo-Riojas, "Prostate-specific antigen (PSA) as a possible biomarker in non-prostatic cancer: a review," *Cancer Epidemiology*, vol. 54, pp. 48–55, 2018.

[4] H. Van Poppel, M. J. Roobol, C. R. Chapple et al., "Prostate-specific antigen testing as part of a risk-adapted early detection strategy for prostate cancer: european association of urology position and recommendations for 2021," *European Urology*, vol. 80, no. 6, pp. 703–711, 2021.

[5] X. P. Liu, N. Chang, J. S. Chen, C. J. Mao, and B. K. Jin, "Ultrasensitive photoelectrochemical immunosensor based on a g-C3N4/SnS2 nanocomposite for prostate-specific antigen detection," *Microchemical Journal*, vol. 168, Article ID 106337, 2021.

[6] Y. C. Chen, M. J. Ruan, B. Y. Zhou et al., "Cutoff values of prostate imaging reporting and data system version 2.1 score in men with prostate-specific antigen level 4 to 10 ng/mL: importance of lesion location," *Clinical Genitourinary Cancer*, vol. 19, pp. 288–295, 2021.

[7] P. Song, B. Yang, Z. Peng et al., "Reduced cancer-specific survival of low prostate-specific antigen in high-grade prostate cancer: a population-based retrospective cohort study," *International Journal of Surgery*, vol. 76, pp. 64–68, 2020.

[8] M. J. Chen, Z. W. Tang, C. B. Ma, and Y. Yan, "A fluorometric aptamer based assay for prostate specific antigen based on enzyme-assisted target recycling," *Sensors and Actuators B: Chemical*, vol. 302, Article ID 127178, 2020.

[9] C. Dejous and U. M. Krishnan, "Sensors for diagnosis of prostate cancer: looking beyond the prostate specific antigen," *Biosensors and Bioelectronics*, vol. 173, Article ID 112790, 2021.

[10] C. Ibau, M. K. Md-Arshad, and S. C. B. Gopinath, "Current advances and future visions on bioelectronic immunosensing for prostate-specific antigen," *Biosensors and Bioelectronics*, vol. 98, pp. 267–284, 2017.

[11] F. Ghorbani, H. Abbaszadeh, J. E. N. Dolatabadi, L. Aghebati-Maleki, and M. Yousefi, "Application of various optical and electrochemical aptasensors for detection of human prostate specific antigen: a review," *Biosensors and Bioelectronics*, vol. 142, Article ID 111484, 2019.

[12] Y. Chang, M. M. Wang, L. Y. Wang, and N. Xia, "Recent progress in electrochemical biosensors for detection of prostate-specific antigen," *International Journal of Electrochemical Science*, vol. 13, pp. 4071–4084, 2018.

[13] H. M. Wang, X. Q. Huang, A. J. Wang et al., "Construction of efficient "on-off-on" fluorescence aptasensor for ultrasensitive detection of prostate specific antigen via covalent energy transfer between g-C3N4 quantum dots and palladium

[14] triangular plates," *Analytica Chimica Acta*, vol. 1104, pp. 53–59, 2020.

[14] H. M. Kim, J. H. Park, D. H. Jeong, H. Y. Lee, and S. K. Lee, "Real-time detection of prostate-specific antigens using a highly reliable fiber-optic localized surface plasmon resonance sensor combined with micro fluidic channel," *Sensors and Actuators B: Chemical*, vol. 273, pp. 891–898, 2018.

[15] S. Gutkin, O. Green, G. Raviv, D. Shabat, and O. Portnoy, "Powerful chemiluminescence probe for rapid detection of prostate specific antigen proteolytic activity: forensic identification of human semen," *Bioconjugate Chemistry*, vol. 31, no. 11, pp. 2488–2493, 2020.

[16] F. Hou, X. B. Hu, S. H. Ma, J. T. Cao, and Y. M. Liu, "Construction of electrochemiluminescence sensing platform within situ generated coreactant strategy for sensitive detection of prostate specific antigen," *Journal of Electroanalytical Chemistry*, vol. 858, Article ID 113817, 2020.

[17] R. Gao, Z. Y. Lv, Y. S. Mao et al., "SERS-based pump-free microfluidic chip for highly sensitive immunoassay of prostate-specific antigen biomarkers," *ACS Sensors*, vol. 4, pp. 938–943, 2019.

[18] F. Farshchi and M. Hasanzadeh, "Nanomaterial based aptasensing of prostate specific antigen (PSA): recent progress and challenges in efficient diagnosis of prostate cancer using biomedicine," *Biomedicine & Pharmacotherapy*, vol. 132, Article ID 110878, 2020.

[19] C. Hu, W. Q. Yue, and M. G. Yang, "Nanoparticle-based signal generation and amplification in microfluidic devices for bioanalysis," *Analyst*, vol. 138, no. 22, p. 6709, 2013.

[20] M. Barani, F. Sabir, A. Rahdar, R. Arshad, and G. Z. Kyzas, "Nanotreatment and nanodiagnosis of prostate cancer: recent updates," *Nanomaterials*, vol. 10, no. 9, p. 1696, 2020.

[21] M. Azharuddin, G. H. Zhu, D. Das et al., "A repertoire of biomedical applications of noble metal nanoparticles," *Chemical Communications*, vol. 55, no. 49, pp. 6964–6996, 2019.

[22] P. M. Martins, A. C. Lima, S. Ribeiro, S. Lanceros-Mendez, and P. Martins, "Magnetic nanoparticles for biomedical applications: from the soul of the earth to the deep history of ourselves," *ACS Applied Bio Materials*, vol. 4, no. 8, pp. 5839–5870, 2021.

[23] L. H. Li, Y. Wei, S. P. Zhang, X. S. Chen, T. L. Shao, and D. X. Feng, "Electrochemical immunosensor based on metal ions functionalized CNSs@Au NPs nanocomposites as signal amplifier for simultaneous detection of triple tumor markers," *Journal of Electroanalytical Chemistry*, vol. 880, Article ID 114882, 2021.

[24] F. Ma, C. C. Li, and C. Y. Zhang, "Development of quantum dot-based biosensors: principles and applications," *Journal of Materials Chemistry B*, vol. 6, no. 39, pp. 6173–6190, 2018.

[25] L. H. Li, D. X. Feng, J. Q. Zhao, Z. L. Guo, and Y. Z. Zhang, "Simultaneous fluoroimmunoassay of two tumor markers based on CdTe quantum dots and gold nanocluster coated-silica nanospheres as labels," *RSC Advances*, vol. 5, no. 128, pp. 105992–105998, 2015.

[26] D. P. Tang, Y. L. Cui, and G. N. Chen, "Nanoparticle-based immunoassays in the biomedical field," *Analyst*, vol. 138, no. 4, p. 981, 2013.

[27] X. H. Lin, A. O. Beringhs, and X. L. Lu, "Applications of nanoparticle-antibody conjugates in immunoassays and tumor imaging," *AAPS*, vol. 43, p. 1550, 2021.

[28] H. Wu, Q. S. Huo, S. Varnum et al., "Dye-doped silica nanoparticle labels/protein microarray for detection of protein biomarkers," *Analyst*, vol. 133, no. 11, p. 1550, 2008.

[29] X. Wu, M. Wu, and J. X. Zhao, "Recent development of silica nanoparticles as delivery vectors for cancer imaging and therapy," *Nanomedicine: Nanotechnology, Biology and Medicine*, vol. 10, no. 2, pp. 297–312, 2014.

[30] V. Shirshahi and M. Soltani, "Solid silica nanoparticles: applications in molecular imaging," *Contraste Media and Molecular Imaging*, vol. 10, p. 1, 2015.

[31] J. Huang, H. Wang, D. P. Li, W. Q. Zhao, L. Y. Ding, and Y. Han, "A new immobilized glucose oxidase using SiO_2 nanoparticles as carrier," *Materials Science and Engineering: C*, vol. 31, no. 7, pp. 1374–1378, 2011.

[32] Y. Vida, M. I. Montanez, D. Collado et al., "Dendrimeric antigen-silica particle composites: an innovative approach for IgE quantification," *Journal of Materials Chemistry B*, vol. 1, no. 24, p. 3044, 2013.

[33] R. Scaffaro, L. G. Botta, G. Lo Re, R. Bertani, R. Milani, and A. Sassi, "Surface modification of poly (ethylene-co-acrylic acid) with amino-functionalized silica nanoparticles," *Journal of Materials Chemistry*, vol. 21, no. 11, p. 3849, 2011.

[34] M. Schwab, "Antibody," in *Encyclopedia of Cancer*, M. Schwab, Ed., Springer, Berlin, Germany, 2011.

[35] L. H. Li, D. X. Feng, and Y. Z. Zhang, "Simultaneous detection of two tumor markers using silver and gold nanoparticles decorated carbon nanospheres as labels," *Analytical Biochemistry*, vol. 505, pp. 59–65, 2016.

[36] Y. X. Li, M. Hong, B. Qiu et al., "Highly sensitive fluorescent immunosensor for detection of influenza virus based on Ag autocatalysis," *Biosensors and Bioelectronics*, vol. 54, pp. 358–364, 2014.